Role of asymmetry parameter and dissipation coefficient of K coordinate in angular distribution of fission fragments

D. Naderi*

Department of Physics, Faculty of Basic Sciences, Razi University, P.O. Box 67149, Kermanshah, Iran

(Received 9 June 2014; revised manuscript received 22 July 2014; published 20 August 2014)

Using multidimensional Langevin equations, we have calculated the angular distribution of fission fragments with nonconstant values for the dissipation coefficient of the K coordinate (the projection of the total angular momentum I onto the symmetry axis of the fissioning nuclear system) for symmetry and asymmetry fission. We investigated the relaxation time of the K coordinate, τ_K, as a function of scission criteria and the asymmetry parameter. Calculations are done for $^{16}\mathrm{O} + {}^{232}\mathrm{Th} \longrightarrow {}^{248}\mathrm{Cf}$, $^{16}\mathrm{O} + {}^{238}\mathrm{U} \longrightarrow {}^{254}\mathrm{Fm}$, and $^{16}\mathrm{O} + {}^{248}\mathrm{Cm} \longrightarrow {}^{264}\mathrm{Rf}$ reactions and obtained results are compared with available experimental data. Our calculations with nonconstant values of the K coordinate show that the agreement between theoretical calculations and experimental data for asymmetry fission is better than that for symmetry fission.

DOI: 10.1103/PhysRevC.90.024614 PACS number(s): 25.85.−w, 05.10.Gg, 24.75.+i

I. INTRODUCTION

One of the interesting problems in the theory of nuclear fission is nuclear dissipation and its effect on different aspects of fission [1–4]. A momentous factor determining the duration of nuclear fission is the dissipation of the kinetic energy of collective nuclear motion [5,6]. Therefore, theoretical analysis of different experimental data related to nuclear dissipation becomes of extreme importance. An observable of fission reaction such as the angular distribution of fission fragments also depends on the durations of the different stages of the evolution of a fissioning system and its analysis makes it possible to obtain information about the mechanism of nuclear dissipation [7].

The transition-state model is usually used in theoretical analysis of the data on the angular distribution of fission fragments [8–10]. The principle of this model consists of the assumption that there is a certain chosen (transition) configuration of a fissioning system that determines the angular distribution of fission fragments. Thus, there are two limiting assumptions on the position of the transition state and, correspondingly, two variants of the transition-state model: the saddle-point transition-state model [8–10] and the scission-point transition-state model [11–13].

The saddle-point transition-state model provides a sensibly exact reproduction of the experimental data on the anisotropy of the fission fragment angular distributions for reactions in which neutrons, ^{3}He ions, and α particles were used as projectiles [8,14]. The compound nuclei formed in such reactions have a temperature of about 1 MeV and low angular momenta. It has been found that the standard saddle-point transition-state model frequently predicted low values of the angular distribution anisotropy for reactions with more massive ions of carbon, oxygen, and heavier ions [14,15], and the experimental data are closer to the values obtained according to the scission-point transition-state model.

It has been shown that experimental values of the anisotropy of angular distributions cannot be described by either the saddle-point or the scission-point transition-state model [16]. In view of this, it was assumed that, in general, an effective transition state that determines the angular distribution of fission fragments lies somewhere between the saddle point and the scission point.

Eremenko and his colleagues [17,18] proposed a fundamentally new dynamical approach to calculating angular distributions without recourse to the concept of a transition state. In this approach, it is proposed to combine a dynamical description of the shape parameters of a fissile nucleus on the basis of Langevins equations with an analysis of the dynamical evolution of the K mode, where K is the projection of the total angular momentum onto the fission axis, with allowance for thermodynamic fluctuations of K in the evolution process. In those studies, the fission process was simulated on the basis of Langevin dynamics, where the distance between the centers of mass of nascent fragments was used as a collective coordinate (no account was taken of a coordinate associated with the neck thickness, and only symmetric fission was considered). Within this approach, experimental data on the anisotropy of angular distributions and on the average multiplicity of prescission neutrons were successfully described for a number of fusion-fission heavy-ion reactions[19].

In this paper we study the angular distribution of fission fragments using four-dimensional Langevin equations with a nonconstant dissipation coefficient of the K coordinate for symmetry and asymmetry fission. The paper is organized as follows. In Sec. II we explain the Langevin equations and theoretical calculations of the angular distribution of fisssion fragments. The obtained results are given in Sec. III. Finally, a summary and a conclusion of our results are presented in Sec. IV.

II. MODEL

In our dynamical calculations we used a well-known (c,h,α) parametrization. In cylindrical coordinates the surface of the nucleus is given by [20,21]

$$\rho_s^2(z) = (c^2 - z^2)(A_s/c^2 + B_{\mathrm{sh}} z^2/c^2 + \alpha z/c), \qquad (1)$$

*d.naderi@razi.ac.ir

where ρ_s and z are radial and parallel coordinates relative to the symmetry axis, respectively. c denotes the elongation parameter. A_s and $B_{\rm sh}$ are defined in Ref. [20]. The neck thickness parameter in a scission point can be defined by

$$h = -1.047c^3 + 4.297c^2 - 6.309c + 4.073. \tag{2}$$

Also, the asymmetry parameter is defined as

$$\alpha = 0.11937\alpha_{\rm as}^2 + 0.24720\alpha_{\rm as}, \tag{3}$$

where

$$\alpha_{\rm as} = \frac{A_1 - A_2}{A}. \tag{4}$$

In this relation A_1 and A_2 are the mass numbers of two fission fragments and A is the mass number of the compound nucleus. In the stochastic approach, evaluation of the collective coordinates is considered as motion of Brownian particles which interact stochastically with a large number of internal degrees of freedom, constituting the surrounding heat bath.

A. Langevin equations

The variation of the orientation degree of freedom (K coordinate) is calculated using the following equation [22,23]:

$$dK = -\frac{\gamma_K^2 I^2}{2}\frac{\partial V}{\partial K}dt + \gamma_K I\sqrt{\frac{Tdt}{2}}\xi(t), \tag{5}$$

where T is the temperature of the heat bath. In these calculations, we neglected the spins of projectile and target nuclei and $I = l$. $\xi(t)$ is a random variable satisfying the relations

$$\begin{aligned} \langle \xi_i \rangle &= 0, \\ \langle \xi_i(t_1)\xi_j(t_2)\rangle &= 2\delta_{ij}\delta(t_1 - t_2). \end{aligned} \tag{6}$$

γ_K is a parameter that controls the coupling between the orientation degree of freedom and the heat bath. This parameter can be calculated as [23,24]

$$\gamma_K = \frac{1}{R_N R_{\rm c.m.}\sqrt{2\pi^3 n_0}}\sqrt{\frac{J_\parallel |J_{\rm eff}| J_R}{J_\perp^3}}, \tag{7}$$

where R_N, $R_{\rm c.m.}$, and n_0 are the neck radius, the distance between the centers of mass of nascent fragments, and the bulk flux in standard nuclear matter (0.0263 MeV zs fm^{-4}), respectively. $J_R = MR_{\rm c.m.}^2/4$, where M is the compound nucleus mass. Also, the effective moment of inertia has the form

$$\frac{1}{J_{\rm eff}} = \frac{1}{J_\parallel} - \frac{1}{J_\perp}, \tag{8}$$

here $J_\parallel$ and $J_\perp$ are the rigid body moments of inertia of the nucleus with respect to the symmetry axis and an axis orthogonal to it, respectively.

The potential energy of the rotating nuclear system depends on K because we have [25]

$$\begin{aligned} V(q,I,K) = {} & E_s^0(Z,A)(B_s(q) - 1) + E_c^0(Z,A)(B_c(q) - 1) \\ & + \frac{\left[I(I+1) - K^2\right]\hbar^2}{2J_\perp} + \frac{K^2\hbar^2}{2J_\parallel}, \end{aligned} \tag{9}$$

where Z is the charge of the fissioning nucleus. E_s^0 and E_c^0 are the surface and the Coulomb energy of a spherical nucleus within the liquid drop model with a sharp edge, respectively. Also, $B_c(q)$ and $B_s(q)$ are the dimensionless Coulomb energies of the spherical system and the surface energies, respectively [25].

We employed the Langevin equations to calculate variations of elongation, neck thickness, and asymmetry parameters with time as [26]

$$\begin{aligned} p_i^{(n+1)} = {} & p_i^{(n)} - \tau\left[\frac{1}{2}p_j^{(n)}p_k^{(n)}\left(\frac{\partial m_{jk}(q)}{\partial q_i}\right)^{(n)} - Q_i^{(n)}(q)\right. \\ & \left. - \gamma_{ij}^{(n)}(q)m_{jk}^{(n)}(q)p_k^{(n)}\right] + \theta_{ij}^{(n)}\xi_j^{(n)}\sqrt{\tau}, \\ q_i^{(n+1)} = {} & q_i^{(n)} + \frac{1}{2}m_{ij}^{(n)}(q)\left(p_j^{(n)} + p_j^{(n+1)}\right)\tau. \end{aligned} \tag{10}$$

Here, q_i and p_i are collective coordinates and momenta conjugate to them, respectively. m_{ij} is the tensor of inertia. γ_{ij} is the friction tensor. $\theta_{ij}\xi_j$ is a random force because θ_{ij} is the random force amplitude. The upper index n shows that the corresponding quantity is calculated at the instant $t_n = n\tau$, where τ is the time step in the integration of the Langevin equations. Q_i is a conservative force and is given by

$$Q_i(q,I,K) = -\left(\frac{\partial F}{\partial q_i}\right)_T. \tag{11}$$

Based on the Fermi gas model, the free energy is given by

$$F(q,I,K,T) = V(q,I,K) - a(q)T^2. \tag{12}$$

$a(q)$ is the level density and can be represented in the form

$$a(q) = a_1 A + a_2 A^{2/3} B_s(q). \tag{13}$$

Here, we use the coefficients $a_1 = 0.073$ MeV^{-1} and $a_2 = 0.095$ MeV^{-1} [27].

Using one-body dissipation we can calculate wall friction by [28]

$$\begin{aligned} \gamma_{{\rm wall}_{ij}}(c < c_{\rm win}) = {} & \frac{\pi}{2}\rho_m \overline{v}\int_{z_{\rm min}}^{z_{\rm max}}\left(\frac{\partial \rho_s^2}{\partial q_i}\right) \\ & \times\left(\frac{\partial \rho_s^2}{\partial q_j}\right)\left[\rho_s^2 + \left(\frac{1}{2}\frac{\partial \rho_s^2}{\partial z}\right)^2\right]^{-1/2} dz, \end{aligned} \tag{14}$$

and for an elongation greater than the point at which a neck is formed in the nuclear system ($c \geqslant c_{\rm win}$), the corresponding

friction tensors can be written as

$$\gamma_{\mathrm{wall}_{ij}}(c \geqslant c_{\mathrm{win}}) = \frac{\pi}{2}\rho_m \bar{\upsilon}\Bigg\{\int_{z_{\min}}^{z_{\mathrm{neck}}}\left(\frac{\partial\rho_s^2}{\partial q_i}+\frac{\partial\rho_s^2}{\partial z}\frac{\partial D_1}{\partial q_i}\right)\left(\frac{\partial\rho_s^2}{\partial q_j}+\frac{\partial\rho_s^2}{\partial z}\frac{\partial D_1}{\partial q_j}\right)\left[\rho_s^2+\left(\frac{1}{2}\frac{\partial\rho_s^2}{\partial z}\right)^2\right]^{-1/2}dz$$
$$+\int_{z_{\mathrm{neck}}}^{z_{\max}}\left(\frac{\partial\rho_s^2}{\partial q_i}+\frac{\partial\rho_s^2}{\partial z}\frac{\partial D_2}{\partial q_i}\right)\left(\frac{\partial\rho_s^2}{\partial q_j}+\frac{\partial\rho_s^2}{\partial z}\frac{\partial D_2}{\partial q_j}\right)\left[\rho_s^2+\left(\frac{1}{2}\frac{\partial\rho_s^2}{\partial z}\right)^2\right]^{-1/2}dz\Bigg\}, \quad (15)$$

$$\gamma_{\mathrm{win}_{ij}}(c \geqslant c_{\mathrm{win}}) = \frac{\pi}{2}\rho_m \bar{\upsilon}\left(\frac{\partial R}{\partial q_i}\frac{\partial R}{\partial q_j}\right)\Delta\sigma,$$

where ρ_m is the mass density of the nucleus, $\bar{\upsilon}$ is the average nucleon speed inside the nucleus, and D_1 and D_2 are the positions of the centers of two parts of the fissioning system relative to the center of mass of the whole system. $z_{\min}$ and $z_{\max}$ are the positions of the left and right ends of the nuclear shape. z_{neck} is the position of the neck plane that divides the nucleus into two parts. $\Delta\sigma$ is the area of the window between two parts of the system and R is the distance between the centers of mass of future fragments.

The chaoticity factor (μ) gives the average fraction of trajectories that are chaotic when sampling is done uniformly over the surface. In other words, the chaoticity is used to express the degree of irregularity in the dynamics of the system. Each such trajectory is identified as a regular or as a chaotic one by considering the magnitude of its Lyapunov exponent over a long time interval [29]. By introducing the chaos into the classical linear response theory for one-body dissipation, the scaled versions of wall friction and window friction are obtained as

$$\gamma_{ij}(c < c_{\mathrm{win}}) = \mu(c)\gamma_{ij}^{\mathrm{wall}}(c < c_{\mathrm{win}}),$$
$$\gamma_{ij}(c \geqslant c_{\mathrm{win}}) = \mu(c)\gamma_{ij}^{\mathrm{wall}}(c \geqslant c_{\mathrm{win}}) + \gamma_{ij}^{\mathrm{win}}(c \geqslant c_{\mathrm{win}}), \quad (16)$$

where the value of μ changes from 0 to 1 as the nucleus evolves from spherical to a deformed shape. Also, the finite difference form of the Langevin equation for the orientational degree of freedom K is

$$K^{(n+1)} = K^{(n)} - \frac{\gamma_K^2 I^2}{2}\frac{\partial V}{\partial K}\tau + \Gamma_K^{(n)}\gamma_K I\sqrt{T\tau}, \quad (17)$$

where Γ_K is a normally distributed random number that has zero mean value and a variance equal to unity. By averaging Eq. (5) one can conclude an equation that has the form

$$\langle K(t)\rangle_{K_0} = K_0 \exp\left[\frac{-\gamma_K^2 I^2\hbar^2}{2J_{\mathrm{eff}}}(t-t_0)\right], \quad (18)$$

which gives the following expression for the relaxation time:

$$\tau_K = \frac{2J_{\mathrm{eff}}}{\gamma_K^2 I^2\hbar^2}. \quad (19)$$

Each Langevin trajectory can lead to fission if it overcomes the fission barrier and reaches the scission point. The scission criteria can be determined using the following relation [30]:

$$c_{\mathrm{sci}} = -2.0\alpha^2 + 0.032\alpha + 2.0917. \quad (20)$$

The initial K value was generated using the Monte Carlo method from uniform distribution in the interval $(-L, L)$. Also, for initial values of dynamical parameters we used $c = 1$, $h = 1.01$, and $\alpha = 0$. It should be noted that Eqs. (10) and (17) are numerically solved simultaneously.

B. Formalism for angular distribution of fission fragments

The angular distribution of fission fragments at the transition state configuration is given by [8,31]

$$W(\theta, I, K) = (I + 1/2)\left|D^I_{M,K}(\theta)\right|^2, \quad (21)$$

where quantum number M is the projection of the total spin I on the space fixed axis and $D^I_{M,K}$ is the symmetric top wave function. θ is the angle with respect to the space fixed axis. Also, in case of zero spin target and projectile nuclei, M is zero.

The angular distribution of fission fragments observed in experiment can be obtained by averaging Eq. (21) over the quantum numbers I and K:

$$W(\theta) = \sum_{I=0}^{\infty}\sigma(I)\sum_{K=I}^{I}P_I(K)W(\theta, I, K), \quad (22)$$

where $\sigma(I)$ is the spin distribution function:

$$\sigma(I) = \frac{2\pi}{k^2}\frac{2I+1}{1+\exp[(I-I_c)/\delta I]}. \quad (23)$$

Here k, I_c, and δI are the wave number, the critical spin for fusion, and the diffuseness, respectively. The K equilibrium distribution is

$$P_I^{\mathrm{eq}}(K) = \frac{\exp\left[-K^2/\left(2K_0^2\right)\right]}{\sum_{K=-I}^{I}\exp\left[-K^2/\left(2K_0^2\right)\right]}. \quad (24)$$

The parameter K_0 determines the width of this distribution

$$K_0^2 = J_{\mathrm{eff}}T/\hbar^2, \quad (25)$$

We can use Eq. (22) for four-dimensional dynamical calculations as

$$W(\theta) = \sum_{I=0}^{\infty}\sigma(I)\sum_{K=I}^{I}P_I(K, t_{\mathrm{sc}})W(\theta, I, K), \quad (26)$$

where $P_I(K, t_{\mathrm{sc}})$ is the dynamical distribution calculated from the four-dimensional model at the scission surface for spin I. The anisotropy of the fission fragment angular distribution is given by

$$A = \frac{W(0^\circ)}{W(90^\circ)}. \quad (27)$$

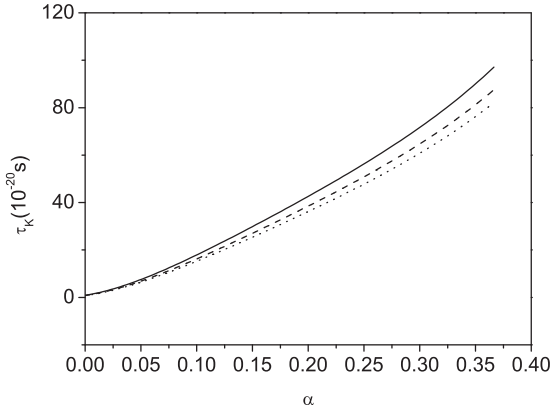

FIG. 1. The relaxation time of the K coordinate, τ_K, as a function of the asymmetry parameter for $I = 80$ at the scission point. Solid, dashed, and dotted lines are the results for $^{16}O + ^{248}Cm \longrightarrow ^{264}Rf$, $^{16}O + ^{238}U \longrightarrow ^{254}Fm$, and $^{16}O + ^{232}Th \longrightarrow ^{248}Cf$ reactions, respectively.

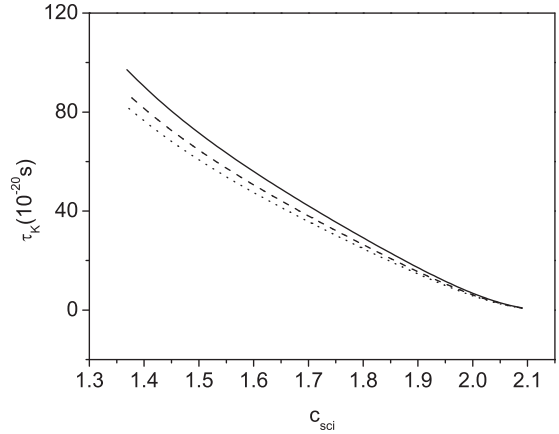

FIG. 2. The relaxation time of the K coordinate, τ_K, as a function of scission criteria for $I = 80$ at the scission point. Solid, dashed, and dotted lines are the results for $^{16}O + ^{248}Cm \longrightarrow ^{264}Rf$, $^{16}O + ^{238}U \longrightarrow ^{254}Fm$, and $^{16}O + ^{232}Th \longrightarrow ^{248}Cf$ reactions, respectively.

It should be noted that in the symmetry fission, the asymmetry degree was frozen at $\alpha = 0$ but for the asymmetry fission we evaluated all Langevin trajectories with $\alpha \neq 0$. In other words, the angular distribution in symmetry and asymmetry fission is calculated, respectively, based on three (c,h,k)- and four (c,h,α,k)-dimensional calculations.

III. RESULTS

To examine the dynamical calculations, we calculated the angular distribution of fission fragments for typical reactions such as $^{16}O + ^{248}Cm \longrightarrow ^{264}Rf$ (at $E_{lab} = 110$, 130, and 148 MeV), $^{16}O + ^{238}U \longrightarrow ^{254}Fm$ (at $E_{lab} = 90$, 130, and 148 MeV), and $^{16}O + ^{232}Th \longrightarrow ^{248}Cf$ (at $E_{lab} = 120$, 140, and 160 MeV). The four-dimensional Langevin equations are applied to calculate the variations of elongation, neck thickness, asymmetry, and K coordinates. The dynamical K distribution has been calculated at the scission point. We used the dissipation coefficient for K as a nonconstant parameter and calculated it as a function of the dynamical parameters. Also, the relaxation time of the Kcoordinate, τ_K, has been calculated as a function of the dynamical parameters.

Figure 1 shows the variation of relaxation time of the K coordinate, τ_K, as a function of the asymmetry parameter for $I = 80$ at the scission point. One can conclude that with the increasing of the asymmetry parameter, the relaxation time of the K coordinate increases. Also, for heavier systems, the relaxation time is higher. The relaxation time of the K coordinate as a function of scission criteria for $I = 80$ at the scission point is shown in Fig. 2. Here, the scission point changes by changing the asymmetry in Eq. (20). With increasing the elongation parameter, the relaxation time decreases. It can be noted that, for a given value of I, the relaxation time of the tilting mode, τ_K, has a strong dependence on the deformation, the asymmetry parameter, and the dissipation coefficient of the K coordinate. Figure 3 demonstrates the dissipation coefficient for the K coordinate as a function of the asymmetry parameter at the scission point for three reactions. We can conclude for symmetry fission ($\alpha = 0$) that the dissipation coefficient has the maximum value, whereas for asymmetry fission with increasing asymmetry parameter, γ_K decreases. The values of the dissipation coefficients for three reactions are similar but with increasing the mass number of the compound nucleus γ_K decreases.

The variation of the anisotropy of the fission fragment angular distribution as a function of energy for three reactions is shown in Fig. 4. We can see for asymmetry fission that the obtained results are in better agrement with experimental data in comparison with the results of symmetry fission. Also, Fig. 4 shows that the values of anisotropy related to asymmetry fission are lower than the obtained results with symmetry fission. Figure 5 displays the angular distribution of fission fragments for the $^{16}O + ^{248}Cm \longrightarrow ^{264}Rf$ reaction at $E_{lab} =$ 110 MeV (a), $E_{lab} = 130$ MeV (b), and $E_{lab} = 148$ MeV (c), respectively. We can see that in lower angles the difference

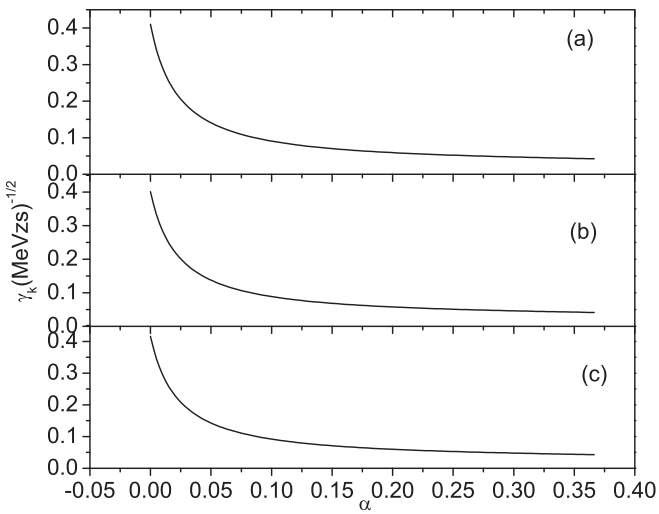

FIG. 3. The dissipation coefficient for K as a function of the asymmetry parameter at the scission point for the $^{16}O + ^{248}Cm \longrightarrow ^{264}Rf$ (a), $^{16}O + ^{238}U \longrightarrow ^{254}Fm$ (b), and $^{16}O + ^{232}Th \longrightarrow ^{248}Cf$ (c) reactions, respectively.

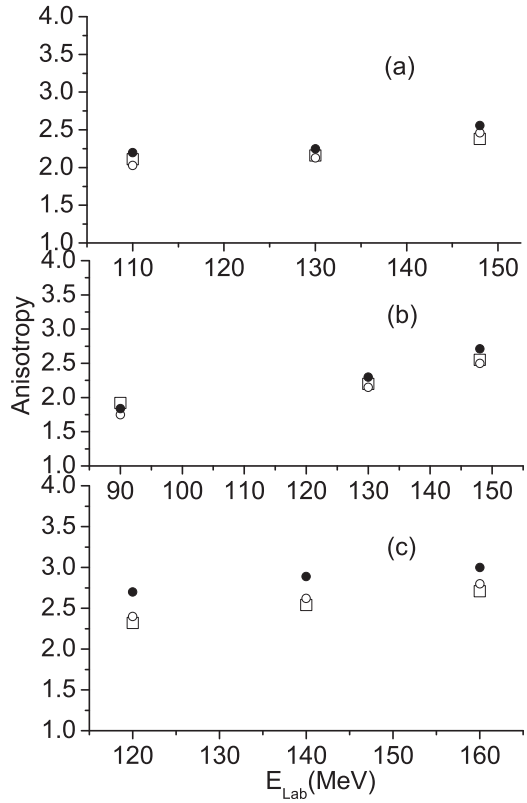

FIG. 4. The anisotropy of the angular distribution of fission fragments as a function of energy for the $^{16}O + ^{248}Cm \longrightarrow ^{264}Rf$ (a), $^{16}O + ^{238}U \longrightarrow ^{254}Fm$ (b), and $^{16}O + ^{232}Th \longrightarrow ^{248}Cf$ (c) reactions, respectively. The open squares are the experimental data [32]. Open and solid circles represent the results based on a nonconstant dissipation coefficient for asymmetry ($\alpha \neq 0$) and symmetry ($\alpha = 0$) fission, respectively.

between the results of symmetry and asymmetry fission is high, whereas in higher angles the difference is low.

The obtained results of angular distribution for the $^{16}O + ^{232}Th \longrightarrow ^{248}Cf$ and $^{16}O + ^{238}U \longrightarrow ^{254}Fm$ reactions are presented in Figs. 6 and 7, respectively. These figures show same results as Fig. 5. The obtained results from theoretical calculations based on asymmetry fission with a nonconstant dissipation coefficient for K are in better agreement with experimental data in comparison with the obtained results based on symmetry fission.

Using Langevin equations we study the relaxation process of the K coordinate and take into account the effect of evaluation of the K value on the dynamics of fission. The distribution $P_I(K,t_{sc})$ at the scission surface is calculated dynamically using Langevin equations. This quantity depends on the dissipation coefficients of the K coordinate and the dynamical parameters. The obtained distribution for $P_I(K,t_{sc})$ in symmetry ($\alpha = 0$) and asymmetry ($\alpha \neq 0$) fission are different from each other. Thus, the angular distribution and consequently the anisotropy in symmetry and asymmetry fission are not equal.

It should be noted that we used the heavy systems in which the mean descent time between the saddle and scission points

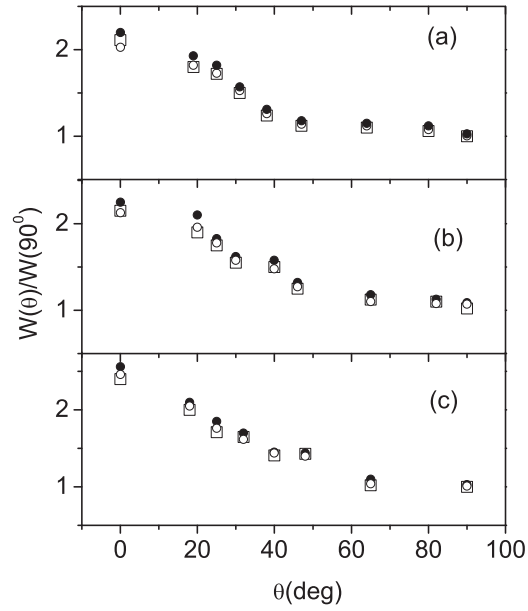

FIG. 5. The angular distribution of fission fragments for the $^{16}O + ^{248}Cm \longrightarrow ^{264}Rf$ reaction at $E_{lab} = 110$ MeV (a), $E_{lab} = 130$ MeV (b), and $E_{lab} = 148$ MeV (c), respectively. The open squares are the experimental data [32]. Open and solid circles represent results with a nonconstant dissipation coefficient for asymmetry ($\alpha \neq 0$) and symmetry ($\alpha = 0$) fission, respectively.

is higher than it is for light systems. Also, for these systems τ_K is comparable with the time between the saddle and scission points and, consequently, the memory of distribution of the

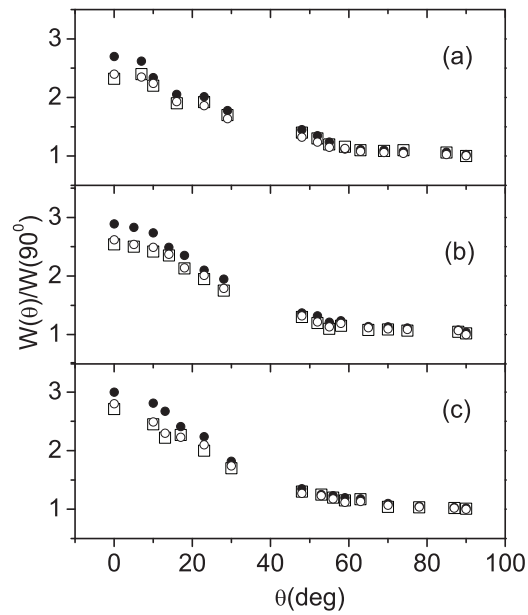

FIG. 6. The angular distribution of fission fragments for $^{16}O + ^{232}Th \longrightarrow ^{248}Cf$ reaction at $E_{lab} = 120$ MeV (a), $E_{lab} = 140$ MeV (b), and $E_{lab} = 160$ MeV (c), respectively. The open squares are the experimental data [32]. Open and solid circles represent results with a nonconstant dissipation coefficient for asymmetry ($\alpha \neq 0$) and symmetry ($\alpha = 0$) fission, respectively.

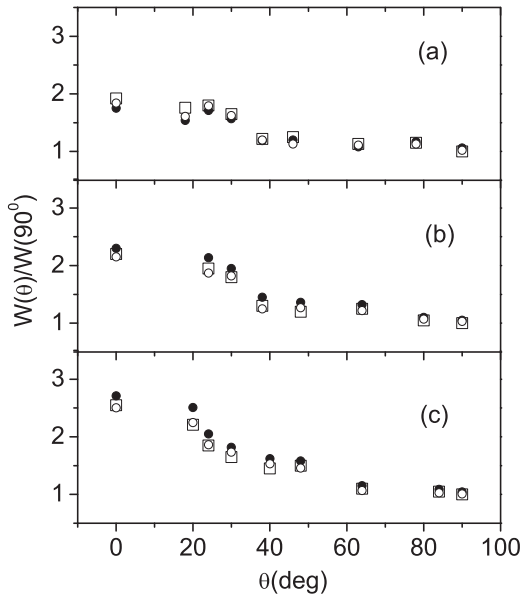

FIG. 7. The angular distribution of fission fragments for $^{16}O + ^{238}U \longrightarrow ^{254}Fm$ reaction at $E_{lab} = 90$ MeV (a), $E_{lab} = 130$ MeV (b), and $E_{lab} = 148$ MeV (c), respectively. The open squares are the experimental data [32]. Open and solid circles represent results with non constant dissipation coefficient based on asymmetry ($\alpha \neq 0$) and symmetry ($\alpha = 0$) fission, respectively.

tilting mode can affect the angular distribution of fission fragments at the scission point.

IV. SUMMARY AND CONCLUSION

In this paper, we calculated the angular distribution of fission fragments dynamically using four-dimensional Langevin equations with a nonconstant dissipation coefficient for the K coordinate. The influence of the asymmetry parameter was investigated by comparison of the dynamical calculation of the angular distribution of fission fragments for symmetry and asymmetry fission. One can conclude that the relaxation time of the tilting mode is dependent on the asymmetry parameter and this quantity in symmetry and asymmetry fission is different. Consequently, by introducing the dependence of the dissipation coefficient for the K coordinate and the relaxation time of the tilting mode on the asymmetry parameter, one can obtain good agreement between theoretical calculations and experimental data for the angular distribution of fission fragments.

In summary, it is necessary to stress that the clarification of the role of the dynamical factors influenced the formation of the angular distribution of fission fragments. The present dynamical approach allowed us to obtain sensible agreement of the results of calculations with experimental angular distributions.

[1] J. O. Newton, Fiz. Elem. Chastits At. Yadra **21**, 821 (1990) [Sov. J. Part. Nucl. **21**, 349 (1990)].
[2] P. Fröbrich and I. I. Gontchar, Phys. Rep. **292**, 131 (1998).
[3] P. Paul, Annu. Rev. Nucl. Part. Sci. **44**, 65 (1994).
[4] M. Beckerman, Rep. Prog. Phys. **51**, 1047 (1988).
[5] G. D. Adeev *et al.*, Fiz. Elem. Chastits At. Yadra **36**, 732 (2005) [Phys. Part. Nucl. **36**, 378 (2005)].
[6] Y. Abe *et al.*, Phys. Rep. **275**, 49 (1996).
[7] D. O. Eremenko *et al.*, J. Phys. G: Nucl. Part. Phys. **22**, 1077 (1996).
[8] R. Vandenbosch and J. R. Huizenga, *Nuclear Fission* (Academic Press, New York, 1973), p. 422.
[9] A. Bohr, in *Proceedings of the United Nations International Conference on the Peaceful Uses of Atomic Energy (New York)* (United Nations, Great Britain, 1956), Vol. 2, p. 151.
[10] I. Halpern and V. M. Strutinsky, in *Proceedings of the Second United Nations International Conference on the Peaceful Uses of Atomic Energy (Geneva)* (United Nations, Great Britain, 1958), Vol. 15, p. 408.
[11] P. D. Bond, Phys. Rev. C **32**, 471 (1985).
[12] H. H. Rossner, J. R. Huizenga, and W. U. Schröder, Phys. Rev. A **33**, 560 (1986).
[13] B. John and S. K. Kataria, Phys. Rev. C **57**, 1337 (1998).
[14] L. C. Vaz and J. M. Alexander, Phys. Rep. **97**, 1 (1983).
[15] A. V. Karpov, R. M. Hiryanov, A. V. Sagdeev, and G. D. Adeev, J. Phys. G: Nucl. Part. Phys. **34**, 255 (2007).
[16] R. Freifelder, M. Prakash, and J. M. Alexander, Phys. Rep. **133**, 315 (1986).
[17] V. A. Drozdov, D. O. Eremenko, O. V. Fotina, S. Yu. Platonov, and O. A. Yuminov, AIP Conf. Proc. **704**, 130 (2004).
[18] D. O. Eremenko, V. A. Drozdov, M. Eslamizadh *et al.*, Phys. At. Nucl. **69**, 1423 (2006).
[19] R. M. Hiryanov, A. V. Karpov, and G. D. Adeev, Phys. At. Nucl. **71**, 1361 (2008).
[20] A. K. Dhara, K. Krishan, C. Bhattacharya, and S. Bhattacharya, Phys. Rev. C **57**, 2453 (1998).
[21] D. Naderi, M. R. Pahlavani, and S. A. Alavi, Phys. Rev. C **87**, 054618 (2013).
[22] P. N. Nadtochy, E. G. Ryabov, A. E. Gegechkori, Y. A. Anischenko, and G. D. Adeev, Phys. Rev. C **85**, 064619 (2012).
[23] J. P. Lestone and S. G. McCalla, Phys. Rev. C **79**, 044611 (2009).
[24] D. Naderi, J. Phys. G: Nucl. Part. Phys. **40**, 125103 (2013).
[25] A. J. Sierk, Phys. Rev. C **33**, 2039 (1986).
[26] Yu. A. Anischenko, A. E. Gegechkori, and G. D. Adeev, Phys. At. Nucl. **74**, 341 (2011).
[27] A. V. Ignatyuk *et al.*, Yad. Fiz. **21**, 1185 (1975) [Sov. J. Nucl. Phys. **21**, 612 (1975)].
[28] D. Naderi, Phys. Rev. C **86**, 044609 (2012).
[29] J. Blocki, F. Brut, T. Srokowski, and W. J. Swiatecki, Nucl. Phys. A **545**, 511 (1992).
[30] M. R. Pahlavani and D. Naderi, Phys. Rev. C **83**, 024602 (2011).
[31] A. Boher and B. R. Mottelson, *Nuclear Structure* (World Scientific, Singapore, 1998), Vol. 2, p. 424.
[32] B. B. Back, R. R. Betts, J. E. Gindler, B. D. Wilkins, S. Saini, M. B. Tsang, C. K. Gelbke, W. G. Lynch, M. A. McMahan, and P. A. Baisden, Phys. Rev. C **32**, 195 (1985).